

nature



WHAT'S IN A NAME?
'Planet' 2003 UB313
weighs in

MALARIA IN AFRICA
Weather forecasts
track epidemic risk

DNA REPLICATION
A new look at
old problems

NATUREJOBS
Mental matters

SPHERICAL VIRUS STRUCTURE

**DNA packaging and injection in
a *Salmonella* phage**



LETTERS

Structure of epsilon15 bacteriophage reveals genome organization and DNA packaging/injection apparatus

Wen Jiang^{1,†}, Juan Chang^{1,2}, Joanita Jakana¹, Peter Weigele³, Jonathan King³ & Wah Chiu^{1,2}

The critical viral components for packaging DNA, recognizing and binding to host cells, and injecting the condensed DNA into the host are organized at a single vertex of many icosahedral viruses. These component structures do not share icosahedral symmetry and cannot be resolved using a conventional icosahedral averaging method. Here we report the structure of the entire infectious *Salmonella* bacteriophage epsilon15 (ref. 1) determined from single-particle cryo-electron microscopy, without icosahedral averaging. This structure displays not only the icosahedral shell of 60 hexamers and 11 pentamers, but also the non-icosahedral components at one pentameric vertex. The densities at this vertex can be identified as the 12-subunit portal complex sandwiched between an internal cylindrical core and an external tail hub connecting to six projecting trimeric tailspikes. The viral genome is packed as coaxial coils in at least three outer layers with ~90 terminal nucleotides extending through the protein core and the portal complex and poised for injection. The shell protein from icosahedral reconstruction at higher resolution exhibits a similar fold to that of other double-stranded DNA viruses including herpesvirus^{2–6}, suggesting a common ancestor among these diverse viruses. The image reconstruction approach should be applicable to studying other biological nanomachines with components of mixed symmetries.

Double-stranded DNA (dsDNA) bacteriophages are vectors for gene transfer among enteric bacteria, including important human pathogens⁷. For all the well-studied tailed dsDNA bacteriophages, a preformed procapsid shell is assembled, and the DNA is pumped into the shell through a portal complex located at a single vertex⁸. The bacteriophage tails are also assembled at this vertex. The portal complex together with packaging enzymes have been shown to function as components of a very powerful molecular motor⁹, but it has not been possible to visualize the complex within the intact virion.

Epsilon15 is a short-tailed dsDNA bacteriophage that infects *Salmonella anatum*. Its genome (NCBI accession number NC_004775) contains 39,671 base pairs with 49 open reading frames (Supplementary Fig. 1). Six gene products, coding for structural proteins, were resolved by SDS–polyacrylamide gel electrophoresis (PAGE) and identified by tryptic-digest/mass spectrometry (Supplementary Fig. 2).

Cryo-electron microscopy of frozen hydrated epsilon15 shows intact particles consisting of isometric heads and a protruding density (Fig. 1a). Approximately 15,000 particle images were used for image reconstruction without symmetry imposition. The 20 Å resolution density map of the whole bacteriophage is shown in Fig. 1b (Supplementary Movie 1). The angular-shaped capsid has a $T = 7I$

shell, with a larger diameter (700 Å) along the icosahedral five-fold axes and a smaller diameter (650 Å) along the three-fold axes. The virion capsid is made up of 11 pentons and 60 hexons.

One of the five-fold vertices is occupied by six tailspikes (red) surrounding an external tail hub (yellow). A cross-section of the reconstruction (Fig. 1c) and cut-away view (Fig. 1d) reveal, inside the capsid shell (dark green), the densities of the portal complex (purple), a protein core (light green) and the packaged viral DNA (blue). Figure 1e shows three well-resolved concentric shells representing the dsDNA packed coaxially around the five-fold axis.

The ~40-kilobase (kb) epsilon15 dsDNA genome has a length of 14 μm in an extended form and needs to assume a compact arrangement when it is packaged into the capsid. This compact arrangement must also be topologically organized to facilitate efficient dsDNA release during infection. The epsilon15 genome structure is sufficiently resolved to see the individual dsDNA strands with a ~25 Å separation for at least the three outermost layers (Fig. 1d, e), which are packed coaxially around the vertical axis in Fig. 1c, d, coincident with the capsid five-fold/portal/tail axis. Neighbouring dsDNA strands are packed hexagonally, which appears to be the most space-efficient and energetically favourable packing pattern for the cylindrically shaped dsDNA strands. The coaxial dsDNA rings are better resolved in the outermost layers closest to the capsid shell than those in the inner layers (Fig. 1c, d). This suggests that the dsDNA packaging starts from the inner surface of the capsid shell (light blue in Fig. 1d, e), spools towards the inner radius region and ends as a terminal shaft in the portal channel (dark blue in Fig. 1d, e). This type of packing agrees qualitatively with the coaxial spooling model based on scattering¹⁰, simulations¹¹ and previous cryo-electron microscopy reconstruction¹². Our observed spool axis is consistent with the T7 spooling model¹³, but orthogonal to an earlier model of T4 (ref. 10), and does not appear to vary in different layers¹¹.

On the surface of the capsid, six tailspikes, composed of gp20, connect to a central tail hub, which extends out from one of the capsid's five-fold vertices (Figs 1b and 2a). This symmetry mismatch with a six-fold tail complex located at a five-fold vertex is a characteristic feature of tailed dsDNA bacteriophages. Each tailspike consists of two structural domains separated by a bend: a capsid proximal stem bound to the central tail hub and a distal flower-like domain composed of three petals around a central knob (Fig. 2a; see also Supplementary Fig. 4b). The distal end of the flower-like domain is clearly trimeric, suggesting a homo-trimer of gp20. These tailspikes bind and cleave the O-antigen component of the host's cell surface lipopolysaccharide¹. The petal-like densities are candidates for this enzymatic function. The bend may represent a functional hinge of

¹National Center for Macromolecular Imaging, Verna and Marrs McLean Department of Biochemistry and Molecular Biology, ²Graduate Program in Structural and Computational Biology and Molecular Biophysics, Baylor College of Medicine, Houston, Texas 77030, USA. ³Department of Biology, Massachusetts Institute of Technology, Cambridge, Massachusetts 02139, USA. †Present address: Department of Biological Sciences, Purdue University, West Lafayette, Indiana 47907, USA.

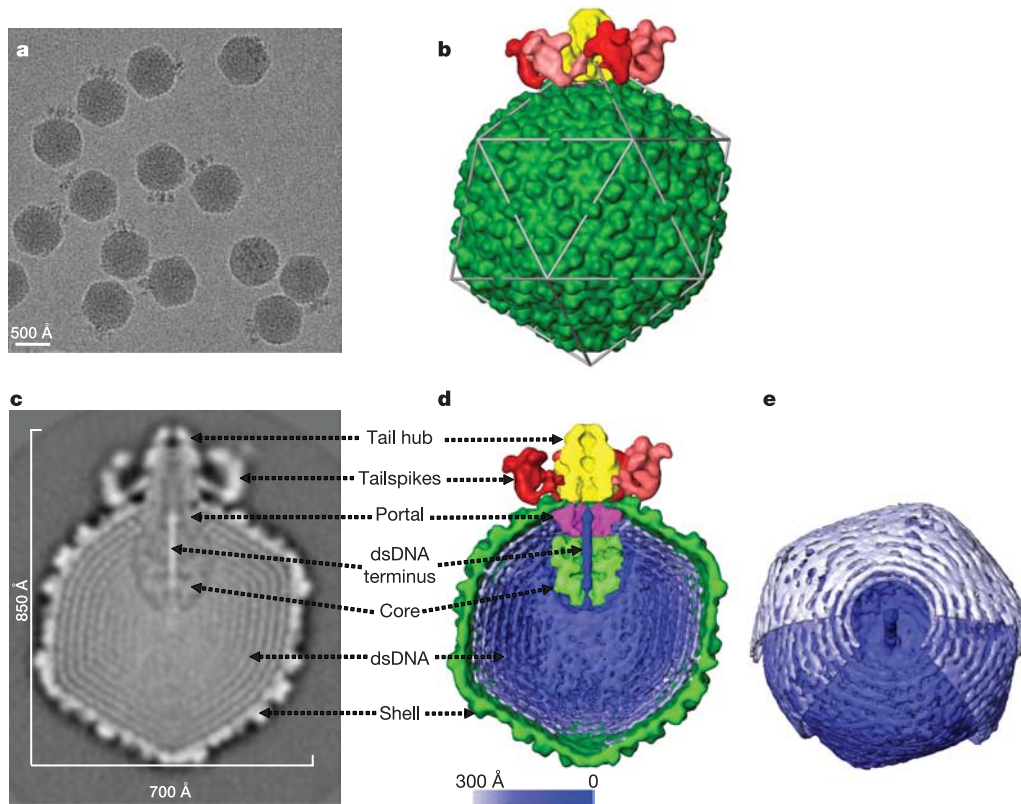


Figure 1 | Structure of epsilon15 bacteriophage. **a**, 200-kV CCD image of epsilon15 particles embedded in vitreous ice. **b**, Surface rendering of the 20 Å resolution three-dimensional map of entire epsilon15 bacteriophage reconstructed without symmetry imposition. The capsid (dark green) exhibits good icosahedral symmetry as indicated by the icosahedral lattice (grey). **c**, **d**, The structural components of epsilon15 bacteriophage are annotated in the central section density (**c**) and the cut-away surface view (**d**) of the three-dimensional density map. Each of the structural components is coloured differently and the same colour scheme is used in Figs 1–3. **e**, A slightly tilted view of the coaxially packed dsDNA genome. Only portions of the first and second layers of dsDNA are shown so that the three outermost layers can be viewed. Colour gradient (light blue to darker blue) is used in **d** and **e** to indicate the likely packaging order of the dsDNA starting from the outer layer towards inner layers and ending as the central straight segment of terminus.

the tailspike that transmits a recognition signal to activate the tail hub for viral genome injection.

The tail deviates from exact six-fold azimuthal symmetry (Fig. 2a, c; see also Supplementary Fig. 4a). Each of the tailspikes has a slightly different orientation (Supplementary Fig. 4a) but similar

conformation, except for tailspike 3 (Supplementary Fig. 4b). These differences among individual tailspikes may arise from the different interaction sites on the capsid shell surface and the symmetry mismatches between the strict five-fold shell and the quasi six-fold tail. Two neighbouring tailspikes (labelled with an asterisk in Fig. 2b)

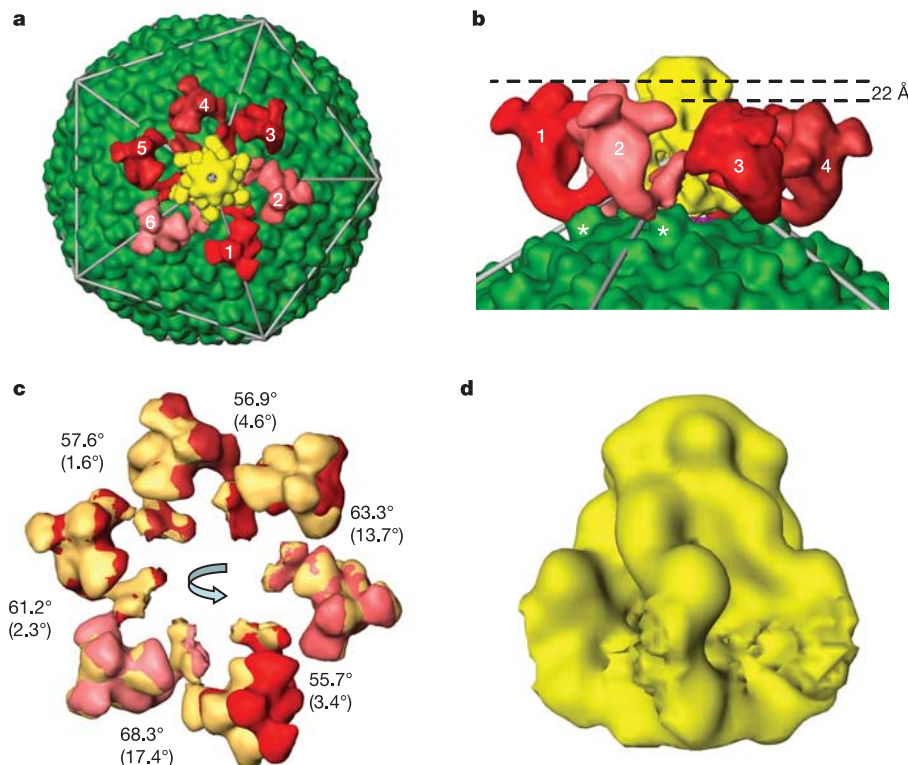


Figure 2 | The tail structure. **a**, Top view of the tail in the epsilon15 reconstruction. Each of the six tailspikes is uniquely coloured with an arbitrary shade of red in order to illustrate the inexact six-fold arrangement around the central tail hub (yellow) with good six-fold symmetry. **b**, Higher-magnification side view of the tailspikes. The contact sites for two (labelled as 1 and 2) out of the six tailspikes are on the capsid surface protrusion densities at local two-fold positions (labelled with an asterisk). **c**, Each of the tailspikes is aligned with its neighbour (anticlockwise) with indicated amount of rotation around an axis that is tilted away from the six-fold axis in different degrees, as indicated in parentheses. The tailspikes in the original positions are displayed in the same shades of red as in **a**, whereas the rotated tailspikes in the new positions are displayed in yellow. **d**, Side view of the tail hub. The segmentation of the tail hub at the interacting regions with the tailspikes is arbitrary because of their tight binding and limited resolution.

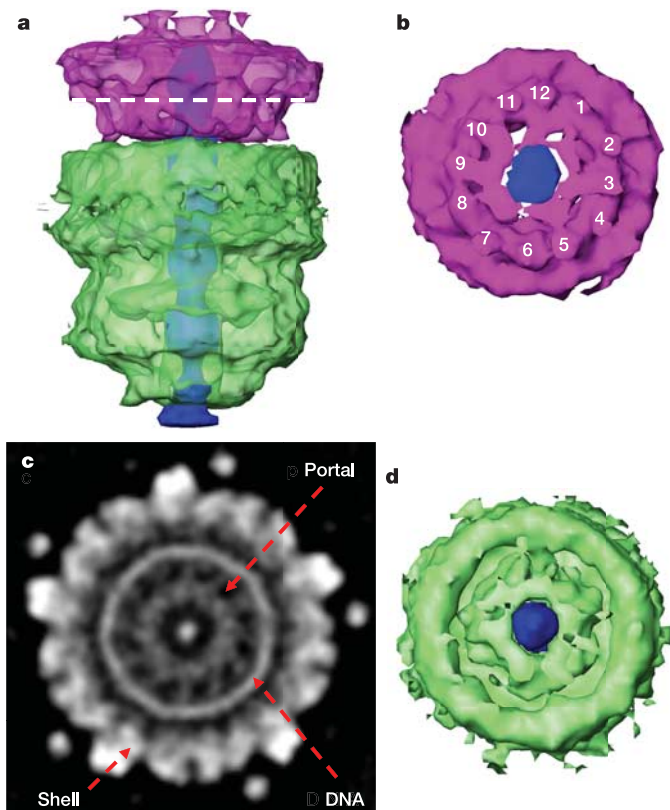


Figure 3 | Structure of the portal complex and internal core. **a**, Side view of the portal complex (pink), internal core (light green) and the putative straight dsDNA terminus (dark blue). The portal complex and internal core are coloured semi-transparently to show that their central channels are filled with the putative dsDNA terminus. **b**, Bottom view of the portal complex with the nearly 12-fold structural features labelled around the filled central channel. **c**, The apparent 12-fold arrangement of densities for the portal complex in a section image of the three-dimensional map. The location of the section is indicated by the dashed line in **a**. **d**, Top view of the internal core (light green) showing the central channel filled with the putative dsDNA terminus (dark blue).

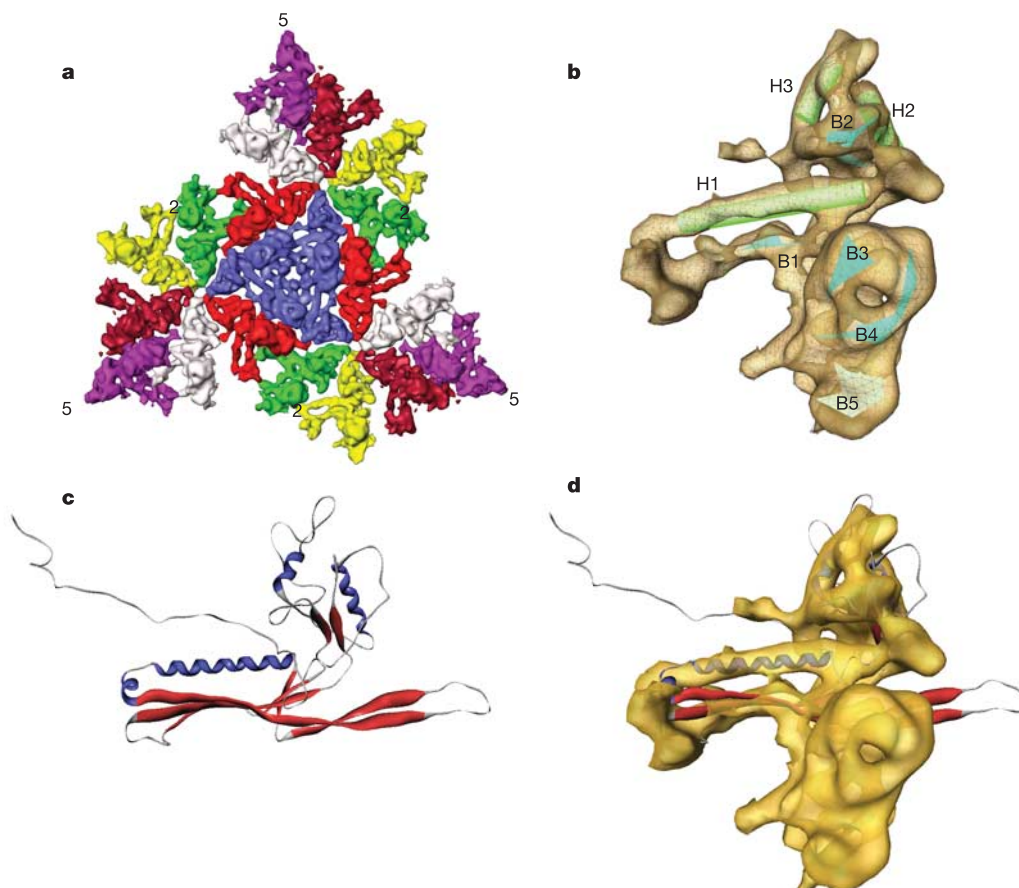


Figure 4 | Shell protein structure. **a**, Surface rendering of three asymmetric units forming one icosahedral face of the $T = 7I$ shell. Each of the seven subunits is coloured differently. **b**, A single averaged shell protein subunit with three helices (H1–H3) and five sheets (B1–B5) annotated. **c**, Ribbon

representation of the atomic model of HK97 head protein gp5 (Protein Data Bank accession 1OHG). Helices are coloured in blue whereas sheets are in red. **d**, Superposition of epsilon15 averaged shell protein subunit and the HK97 head protein gp5.

contact the protrusions at the local two-fold positions of the shell, whereas the other four spikes have tenuous interactions with the shell at different locations at smaller radii. The two elevated contact points force these two tailspikes to a higher radius by 22 Å than the other four tailspikes, and result in a slight overall tilt of the tail (Fig. 2b).

At the centre of the six tailspikes is the tail hub of size ~ 170 Å (height) by 140 Å (width) (Fig. 2d). The tail hub has good six-fold symmetry (Fig. 2a). It appears to anchor the tailspikes as well as cap the central opening of the portal to prevent premature DNA leakage. Upon binding to the surface of the host cell by the distal petal region of the tailspikes, the induced conformational changes might trigger the opening of the capped central channel (Fig. 1c, d), allowing for DNA injection into the host cell in a manner analogous to a gated ion channel.

Just below the tail hub lays the portal. Although the oligomeric state of portals within intact bacteriophages has long been thought to be 12, it has not been measured until now. Our epsilon15 density map provides unambiguous structural evidence that there are 12 densities at the portal *in situ* (Figs 1c, d and 3a–c; see also Supplementary Fig. 5a, b), which is consistent with previous studies of portal complexes biochemically extracted from bacteriophage particles^{14,15}.

Circumscribed by a well-resolved dsDNA ring, the portal has the appearance of 12 well-resolved turbine-like densities (180 Å in diameter) with nearly equivalent angular spacing (Fig. 3c; see also Supplementary Fig. 5a). This overall feature resembles that seen in other isolated portals with negligible sequence similarity^{16–19}. The azimuthal density distribution of the epsilon15 portal deviates noticeably from perfect 12-fold symmetry (Fig. 3c; see also Supplementary Fig. 5a). The asymmetry of the portal ring may be caused by the non-equivalent interactions between the twelve portal subunits and the five surrounding shell protein subunits.

These observations require that the portal complex has the same spatial relationship with the tailspikes, tail hub and the shell, from particle to particle, implying that there are specific interactions among these components. Otherwise, the portal structure would not be resolved by averaging $\sim 15,000$ varying bacteriophage particles.

Figure 3a, d shows an internal density (light green) organized immediately internal to the portal complex. This feature is ~ 200 Å in height and ~ 180 Å in width without obvious symmetry. We interpret this to be a protein core reminiscent of the bacteriophage T7 internal eight-fold-symmetric structure observed in electron micrographs²⁰. The lack of obvious symmetry for the epsilon15 core could be authentic or result from an azimuthal variation of the core among particles. The epsilon15 capsid volume can accommodate up to 90 kb dsDNA. Because the epsilon15 genome is only ~ 40 kb, there is ample space for a protein core of this size in the capsid chamber. The protein core may facilitate the topological ordering of the dsDNA genome during packaging and/or release as suggested for the T7 core²¹.

A long, straight segment of uniform density (~ 310 Å in length and ~ 30 Å in width) extends from near the capsid centre along the five-fold capsid–tail axis. Because these densities are significantly higher than those of the surrounding protein core and portal complex (Fig. 1c, d), we interpret this segment of density to be the ‘last-in’ segment of packaged dsDNA (~ 90 base pairs). It appears to be poised for release and injection into host cell during infection.

This dsDNA terminus passes through the central opening of the portal and ends slightly beyond the portal to where it is capped by densities closing the tail hub’s central channel (Fig. 1c, d). The observation that epsilon15’s portal channel is filled with a straight segment of putative dsDNA terminus is consistent with the observation that bacteriophage SPPI’s terminal segment of packaged dsDNA is tightly associated with its portal protein²².

Imposing the icosahedral symmetry, a 9.5 Å density map was generated from a separate data set imaged to give a higher resolution reconstruction (Supplementary Movie 2 and Supplementary Figs 3b and 6a, b). This map is sufficiently resolved to delineate the

molecular boundaries of each capsid protein subunit and the secondary structure elements (Fig. 4a, b). In the average subunit map, three helices could be identified (Fig. 4b). Helix H1 is ~ 40 Å long and extends towards the three-fold axes where three neighbouring capsomeres interact intimately (Fig. 4a; see also Supplementary Fig. 8b). Parallel to helix H1 is a large β -sheet that contributes significantly to the local three-fold interactions. The two shorter helices (H2 and H3) are located at the interfaces of adjacent subunits within the same hexon and are nearly parallel to each other.

The dispositions of the helices and sheets are similar to those observed in other bacteriophages and herpesvirus^{2–6} (Fig. 4c, d; see also Supplementary Fig. 7) despite little sequence identity. The similarity extends beyond the protein fold of individual subunits to the molecular interaction patterns between the subunits of a hexon or penton, and at the local three-fold symmetry axes where three neighbouring capsomeres meet (Supplementary Fig. 8a, b). The similarities of the protein fold and assembly of the capsid shell of these viruses suggest that these viruses share an ancient common ancestor and that the capsid protein fold and molecular interactions used to hold the icosahedral shell intact have been strongly conserved during evolution.

METHODS

See Supplementary Methods for further methodological details.

The epsilon15 bacteriophage particles were purified from infected *Salmonella anatum* bacterial culture using gradient centrifugation. The purified bacteriophage particles were prepared for cryo-electron microscopy by rapid freeze plunging²³. The images (Fig. 1a) for the reconstruction without symmetry imposition were recorded on a Gatan 4kx4k CCD camera using the JAMES imaging system²⁴ attached to a JEM2010F microscope operated at 200 kV with a Gatan liquid nitrogen specimen cryo-holder. The images (Supplementary Fig. 6a) for the icosahedral reconstruction at higher resolution were taken in a JEM3000SFF microscope operated at 300 kV and at liquid helium specimen temperature. These images were recorded on KODAK SO163 films and were digitized using a Nikon Super CoolScan 9000 ED scanner.

In both sets of data, the individual bacteriophage particle images were pre-processed with the standard procedures. The SAVR software package²⁵ was used to reconstruct the three-dimensional maps assuming icosahedral symmetry for both data sets. The icosahedral symmetry was further relaxed to C_1 symmetry to generate the reconstruction without symmetry imposition using a set of newly developed programs within the EMAN package²⁶. The 20 Å resolution map without any symmetry imposition was generated using $\sim 15,000$ particle images from ~ 950 CCD frames of the 200-kV data set. The 9.5 Å map with icosahedral symmetry imposition was generated using $\sim 6,000$ particle images from ~ 200 micrographs of the 300-kV data set.

Amira (<http://www.amiravis.com>) visualization software was used for most of the segmentation and graphics displays. Alignment and similarity comparison of the individual subunits of the shell protein were performed using the foldhunter program²⁷. Identification of α -helices and β -sheets was performed using the AIRS program, which provides a graphic interface to the ssehunter program²⁷ in the Chimera visualization software package²⁸.

Received 17 August; accepted 23 November 2005.

1. McConnell, M., Reznick, A. & Wright, A. Studies on the initial interactions of bacteriophage epsilon15 with its host cell, *Salmonella anatum*. *Virology* **94**, 10–23 (1979).
2. Jiang, W. *et al.* Coat protein fold and maturation transition of bacteriophage P22 seen at subnanometer resolutions. *Nature Struct. Biol.* **10**, 131–135 (2003).
3. Wikoff, W. R. *et al.* Topologically linked protein rings in the bacteriophage HK97 capsid. *Science* **289**, 2129–2133 (2000).
4. Fokine, A. *et al.* Structural and functional similarities between the capsid proteins of bacteriophages T4 and HK97 point to a common ancestry. *Proc. Natl Acad. Sci. USA* **102**, 7163–7168 (2005).
5. Morais, M. C. *et al.* Conservation of the capsid structure in tailed dsDNA bacteriophages: the pseudoatomic structure of phi29. *Mol. Cell* **18**, 149–159 (2005).
6. Baker, M. L., Jiang, W., Rixon, F. J. & Chiu, W. Common ancestry of herpesviruses and tailed DNA bacteriophages. *J. Virol.* **79**, 14967–14970 (2005).
7. Breitbart, M., Rohwer, F. & Abedon, S. T. in *Phages: their Role in Bacterial Pathogenesis and Biotechnology* (eds Waldor, M. K., Friedman, D. I. & Adhya, S. L.) 66–91 (ASM Press, Washington DC, 2005).

8. Bazinet, C. & King, J. The DNA translocating vertex of dsDNA bacteriophage. *Annu. Rev. Microbiol.* **39**, 109–129 (1985).
9. Smith, D. E. *et al.* The bacteriophage straight phi29 portal motor can package DNA against a large internal force. *Nature* **413**, 748–752 (2001).
10. Earnshaw, W. C., King, J., Harrison, S. C. & Eiserling, F. A. The structural organization of DNA packaged within the heads of T4 wild-type, isometric and giant bacteriophages. *Cell* **14**, 559–568 (1978).
11. Arsuaga, J., Tan, R. K., Vazquez, M., Summers de, W. & Harvey, S. C. Investigation of viral DNA packaging using molecular mechanics models. *Biophys. Chem.* **101–102**, 475–484 (2002).
12. Zhang, Z. *et al.* Visualization of the maturation transition in bacteriophage P22 by electron cryomicroscopy. *J. Mol. Biol.* **297**, 615–626 (2000).
13. Cerritelli, M. E. *et al.* Encapsidated conformation of bacteriophage T7 DNA. *Cell* **91**, 271–280 (1997).
14. Lurz, R. *et al.* Structural organisation of the head-to-tail interface of a bacterial virus. *J. Mol. Biol.* **310**, 1027–1037 (2001).
15. Carazo, J. M., Fujisawa, H., Nakasu, S. & Carrascosa, J. L. Bacteriophage T3 gene 8 product oligomer structure. *J. Ultrastruct. Mol. Struct. Res.* **94**, 105–113 (1986).
16. Simpson, A. A. *et al.* Structure of the bacteriophage phi29 DNA packaging motor. *Nature* **408**, 745–750 (2000).
17. Orlova, E. V. *et al.* Structure of a viral DNA gatekeeper at 10 Å resolution by cryo-electron microscopy. *EMBO J.* **22**, 1255–1262 (2003).
18. Agirrezabala, X. *et al.* Structure of the connector of bacteriophage T7 at 8 Å resolution: structural homologies of a basic component of a DNA translocating machinery. *J. Mol. Biol.* **347**, 895–902 (2005).
19. Tang, L., Marion, W. R., Cingolani, G., Prevelige, P. E. & Johnson, J. E. Three-dimensional structure of the bacteriophage P22 tail machine. *EMBO J.* **24**, 2087–2095 (2005).
20. Cerritelli, M. E. *et al.* A second symmetry mismatch at the portal vertex of bacteriophage T7: 8-fold symmetry in the procapsid core. *J. Mol. Biol.* **327**, 1–6 (2003).
21. Molineux, I. J. No syringes please, ejection of phage T7 DNA from the virion is enzyme driven. *Mol. Microbiol.* **40**, 1–8 (2001).
22. Tavares, P., Lurz, R., Stiege, A., Ruckert, B. & Trautner, T. A. Sequential headful packaging and fate of the cleaved DNA ends in bacteriophage SPP1. *J. Mol. Biol.* **264**, 954–967 (1996).
23. Dubochet, J. *et al.* Cryo-electron microscopy of vitrified specimens. *Q. Rev. Biophys.* **21**, 129–228 (1988).
24. Booth, C. R. *et al.* A 9 Å single particle reconstruction from CCD captured images on a 200 kV electron cryomicroscope. *J. Struct. Biol.* **147**, 116–127 (2004).
25. Jiang, W. *et al.* Semi-automated icosahedral particle reconstruction at sub-nanometer resolution. *J. Struct. Biol.* **136**, 214–225 (2001).
26. Ludtke, S. J., Baldwin, P. R. & Chiu, W. EMAN: semiautomated software for high-resolution single-particle reconstructions. *J. Struct. Biol.* **128**, 82–97 (1999).
27. Jiang, W., Baker, M. L., Ludtke, S. J. & Chiu, W. Bridging the information gap: computational tools for intermediate resolution structure interpretation. *J. Mol. Biol.* **308**, 1033–1044 (2001).
28. Pettersen, E. F. *et al.* UCSF Chimera—a visualization system for exploratory research and analysis. *J. Comput. Chem.* **25**, 1605–1612 (2004).

Supplementary Information is linked to the online version of the paper at www.nature.com/nature.

Acknowledgements We acknowledge the support of grants from National Institutes of Health and the Robert Welch Foundation. We thank M. Dougherty for the production of the animations, M. Baker for the AIRS program for secondary structure element identification, and M. F. Schmid and F. Rixon for discussions.

Author Contributions W.J. developed the image processing methods and solved and analysed the structures; J.C. and J.J. collected the 200- and 300-kV image data respectively; P.W. did the biochemical preparation and analysis; and W.J., P.W., J.K. and W.C. interpreted the structure and wrote the manuscript.

Author Information The three-dimensional density maps have been deposited into the EBI-MSD EMD database with accession codes EMD-1175 for the complete structure without symmetry imposition and EMD-1176 for the icosahedral shell structure. Reprints and permissions information is available at npg.nature.com/reprintsandpermissions. The authors declare no competing financial interests. Correspondence and requests for materials should be addressed to W.C. (wah@bcm.edu).